6

Magnetic Field Sensors Based on Microelectromechanical Systems (MEMS) Technology

Maria Teresa Todaro[1], Leonardo Sileo[1,2] and Massimo De Vittorio[1,2,3]
[1]*National Nanotechnology Laboratory (NNL), Istituto Nanoscienze-CNR*
[2]*Center for Biomolecular Nanotechnologies UNILE, Istituto Italiano di Tecnologia*
[3]*University of Salento, Lecce*
Italy

1. Introduction

In the last decades magnetic field sensors have been developed and realized for analyzing and controlling thousands of functions (Ripka, 2001), and they have become a widespread presence in modern lifestyle. Numerous applications in different fields of science, engineering, and industry rely on the performance, ruggedness, and reliability of magnetic field sensors.

The applications of magnetic sensors depend on magnetic field dynamic range and resolution and include position sensing, speed detection, current detection, non-contact switching, space exploration, vehicle detection, electronic compasses, geophysical prospecting, non-distructive testing, brain function mapping (Lenz & Edelstein, 2006).

Nowdays there is an increasing requirement for magnetic devices with improved sensitivity and resolution, trying to keep as low as possible their cost and power consumption. Additionally there is the need to develop compact devices with several sensors able to measure different parameters including magnetic field, pressure, temperature, acceleration. In this way a multifunctional device could be integrated on the same substrate containing transducers and electronic circuits in a compact configuration without affecting device performances.

In this context microelectromechanical systems (MEMS) technologies play a prominent role for the development of a new class of magnetic sensors.

In general MEMS devices are miniaturized mechanical systems produced using fabrication techniques already explored in the electronics industry. The exploitation of MEMS technology for device fabrication not only makes possible the reduction of the device dimensions on the order of micrometers, but also allows the integration of the mechanical and electronic components on a single chip. In addition to the small device size this involves other important advantages such as light weight, minimum power consumption, low cost, better sensitivity and high resolution. This technology was successfully employed for the realization of portable devices such as gyroscopes (Chang et al., 2008), accelerometers (Li et al., 2011), micromirrors (Singh et al., 2008), and pressure sensors (Mian & Law, 2010).

Magnetic field sensors based on MEMS technology, depending on their operation principle and magnetic range, have a great potential for numerous applications in several fields spanning from vehicle detection and control to mineral prospecting and metal detection as well as to non-distructive testing and medical diagnostics.

This paper aims at the description of current research status in magnetic field sensors focusing on devices fabricated by exploiting MEMS technologies. The paper presents advances in the classes of devices that take advantage from these technologies to scale down magnetic sensors size, namely resonant sensors, fluxgate sensors and Hall sensors.

Resonant sensors exploit Lorentz force principle on micromachined structures excited at one of their resonating modes. These sensors can detect magnetic fields with sensitivity up to 1 T and a maximum achievable resolution of 1 nT.

Fluxgate sensors are inductively working sensors consisting of excitation and sensing coils around a ferromagnetic core. Such sensors can detect static and low frequency magnetic fields up to approximately 1 mT with a maximum resolution of 100 pT.

Hall sensors are based on Hall effect transduction principle and measure either constant or varying magnetic field. They have a magnetic field sensitivity range from 1μT to 1T.

Following the introduction, the paper is organized as follows. The second section, is devoted to the resonant sensors, including the Lorentz force operation principle, examples of realized devices reported in the literature with an highlight on the employed technologies for the fabrication. Third section is focused on fluxgate microsensors including operation principle, state of the art and involved fabrication technologies. Fourth section is dedicated to the description of the Hall effect and Hall magnetic sensors employing MEMS technologies are reported. The fifth section describes the possible applications of this new class of compact devices. Finally in the section sixth the paper ends with the conclusion.

2. Resonant magnetic sensors

Resonant sensors exploit Lorentz force of resonating micromachined structures. These sensors can detect magnetic fields up 1 mT with a resolution down to 1 nT. Such devices are normally based on MEMS technologies, are small in size (order of millimetres), and promise all the advantages related to the employment of fabrication microtechnologies including multifuntionalities and integration of mechanical and electronic components on a single chip.

Resonant magnetic field sensors use resonant structures that are excited at their resonant frequencies by Lorentz forces. Such devices are able to give an amplified response if excited at frequencies equal to the resonant frequencies or vibrational modes of the structures (Bahreyni, 2008).

These structures commonly consist of clamped-free beams or clamped-clamped beams or torsion/flexion plates. In figure 1 it is shown a schematic diagram of the Lorentz force principle acting on a clamped-clamped beam resonant structure. This device can be designed for example to resonate to its first resonant frequency, associated to its first flexural vibration mode. This beam, exposed to an excitation source with a frequency equal to its first resonant frequency, will have a maximum deflection at its midpoint. In order to

excite the device a metallic loop is placed on the clamped-clamped beam surface where an excitation current (I) flows inside it with a frequency equal to the first resonance frequency. When the beam is exposed to an external magnetic field (B_x) in the x-direction, then a Lorentz force (F_L) is generated.

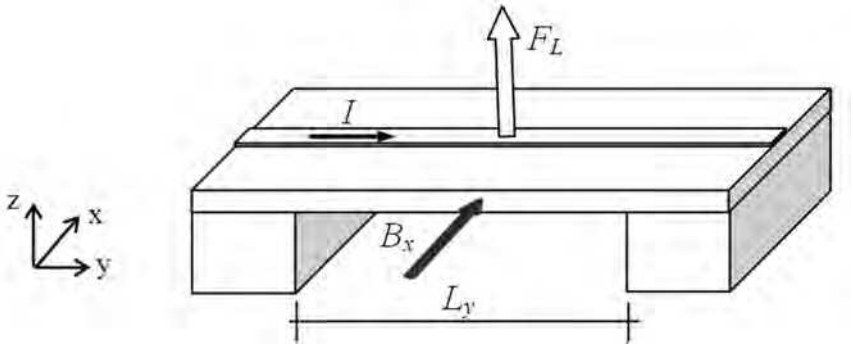

Fig. 1. Schematic diagram of the Lorentz force principle acting on a clamped-clamped beam.

This force can be determined as:

$$F_L = IB_xL_y \tag{1}$$

where the flowing current can be expressed as:

$$I = \sqrt{2}I_{rms}\sin(2\pi ft) \tag{2}$$

where L_y is the length of the metallic loop perpendicular to the magnetic field, I_{rms} is the root mean square of the current I, f is the frequency and t is the time.

The Lorentz force acts as an excitation source on the clamped-clamped beam, causing an amplified deflection on the midpoint. Thus, the magnitude of the beam deflection depends on the Lorentz force amplitude, which is directly proportional to I and B_x.

The application of an external magnetic field alters deflection/torsion of resonating structures with different shapes that is detected by exploiting different readout techniques.

In fact such deflections/torsions result in strain which is related to the elastic modulus of the structure material, to the geometrical characteristics of the resonating structures and to the quality factor (Herrera-May et al. 2010).

The quality factor is an important parameter of the resonant structures. It defines the bandwidth of the resonator relatively to its central resonant frequency or equivalently it expresses the maximum amplitude of the bending structure taking into account the different damping sources (Elwenspoek & Wiegerink, 2001, Beeby et al., 2004). High quality factors involve better device performance, better resolution and improved insensitivity to the disturbances (Beeby et al., 2004).

Another parameter of interest in resonant structures is the resonance frequency. Its determination can be obtained by using both analytical models and simulation tools and

depends on elastic modulus, density, deflection and geometrical features of the resonant structure.

Moreover resonance frequencies are affected by residual stresses on the structure (Weaver et al. 1990). For example thermal stresses inside resonant devices (Hull, 1999) causes strains in the structures which in turn involve (Sabaté et al., 2007) a shift of the resonant frequency of the structures.

Such sensors are typically fabricated in silicon and polysilicon and main disadvantage of this technology is the resonance frequency shift due to temperature changes and environmental pressure which requires compensation electronic circuits and packaging under vacuum respectively.

To detect deflection of resonant structures different readout techniques have been used including the employment of piezoresistive, optical or capacitive techniques.

Piezoresistive sensing exploits changes in the resistance of piezoresistive elements placed in the hinges of the resonant structure, to detect changes in the output voltage signal as effect of strains originating from motions of beams or plates due to the Lorentz force.

Herrera-May et al. (2009) reported on a magnetic field microsensor based on a silicon resonant microplate (400 × 150 × 15 μm^3) and four bending microbeams (130 × 12 × 15 μm^3).

Figure 2 shows a schematic diagram of the fabrication process of the device.

The fabrication process is based on bulk micromachining technology on (100) 4" silicon-on-insulator (SOI) wafers. The process starts by growing a thin thermal oxide layer and depositing a silicon nitride layer on a SOI n-type substrate. The nitride layer is removed from the front side of the wafer and is patterned on the backside (figure 2(a)). Using a second mask, boron is implanted to create four p-type piezoresistors (figure 2(b)). A 1 µm-thick oxide layer is then grown and patterned. The area contacts (120 x 120 μm^2) are opened (figure 3(c)) and then an aluminum layer is deposited and patterned to define metallic lines and pads (figure 4(d)). At this time the silicon substrate is etched from the backside using KOH that stops at the SOI buried oxide (figure 2(e)), which is then removed.

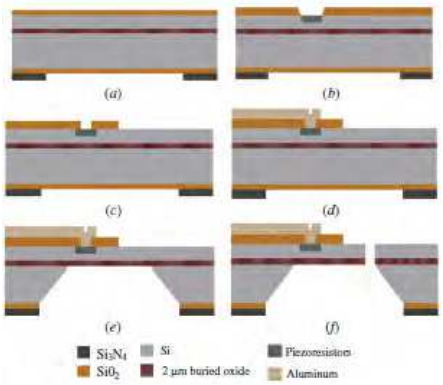

Fig. 2. Schematic diagram of the fabrication process of a piezoresistive resonant magnetic sensor reported by Herrera-May et al. (2009)

Finally, the SOI layer is etched by reactive ion etching (figure 2(f)) to define the plate-beam structure.

Figure 3 shows a schematic design of the resonant magnetic field microsensor reported by Herrera-May et al. (2009) with an highlight on the plate-beam structure and its working principle.

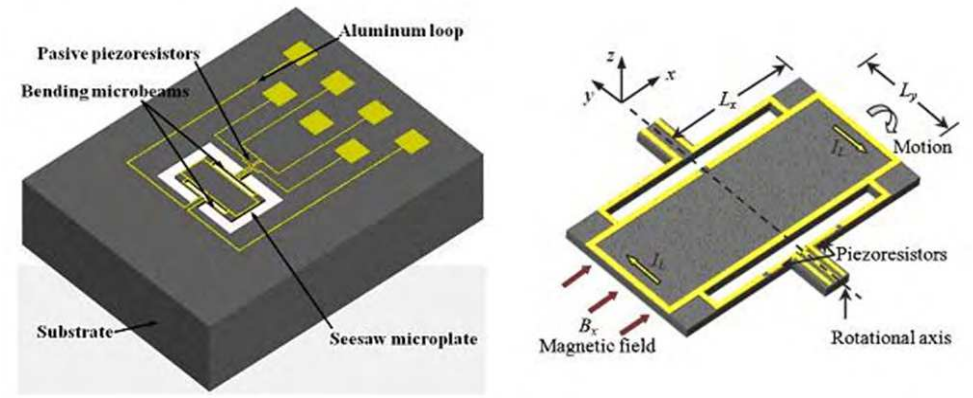

Fig. 3. Schematic design of resonant magnetic field microsensor (left) and highlight on the plate-beam structure and its working principle (right) reported by Herrera-May et al. (2009).

One of the main elements of this sensor is the aluminum rectangular loop deposited on the silicon plate. The Lorentz force causes a seesaw motion on the microplate and the bending of microbeams. Four piezoresistors (p-type) are connected in a Wheatstone bridge and two of these are active piezoresistors located on the microbeams. The Lorentz force originates a longitudinal strain on the two active piezoresistors changing their resistance. The change in the resistance of the active piezoresistors produces an output voltage shift of the Wheatstone bridge.

This sensor has a resonant frequency of 136.52 kHz, a quality factor of 842 at ambient pressure, a sensitivity of 0.403 $\mu V \mu T^{-1}$, a resolution of 143 nT with a frequency variation of 1 Hz, and power consumption below 10 mW. However, the sensor registered an offset and linearity problems in the low magnetic field range.

Tapia et al. (2011) reported on a piezoresistive resonant magnetic microsensor with seesaw rectangular loop of beams reinforced with transversal and longitudinal beams. This device was designed to be compact and to have high resolution for neurobiological applications. Characteristics of this microsensor are a resonant frequency of 13.87 kHz with a quality factor of 93, a resolution of 80 nT, a sensitivity of 1.2 VT^{-1} and a power consumption of 2.05 mW at ambient pressure. This sensor requires a simple signal processing circuit.

Other examples of piezoresistive magnetic sensors on the microscale have been reported in the literature (Beroulle et al. (2003), Sunier et al. (2006)).

Among the resonant magnetic sensors, there are some of them exploiting the optical detection.

Keplinger et al. (2004) reported a resonant magnetic field sensor using U-shaped silicon microbeams and an optical readout system. Figure 4 shows a schematic sketch of the device reported by these authors.

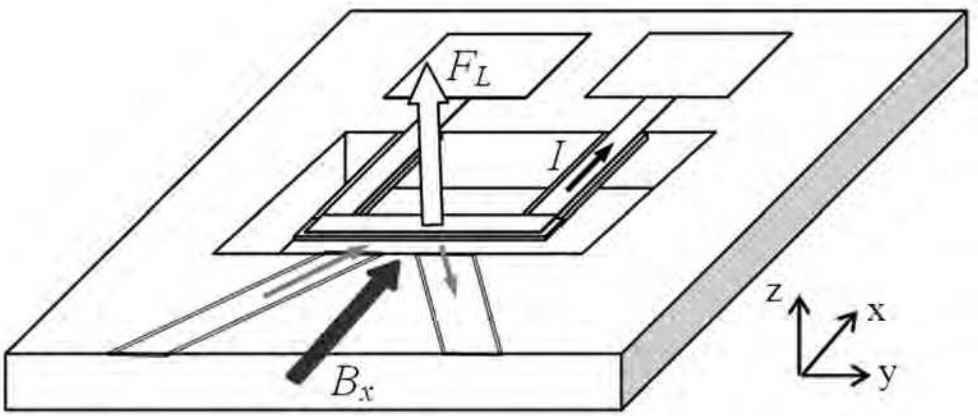

Fig. 4. Schematic sketch of the resonant magnetic sensor with optical readout reported by Keplinger et al. (2004).

Devices are processed by both surface micromachining and bulk micromachining techniques. The etching process has been also used to form the groove for the optical fibers. The microbeams contain a gold loop with a thickness of 500 nm. A magnetic field and an ac electrical current generate a Lorentz force, which bends the microbeams. These deflections are measured by optical sensing using an arrangement consisting of two fibers to avoid interference of reflected light. Figure 4 shows a design, in which the emitted light beam is reflected only once at the microbeam front side. This sensor can measure magnetic fields from 10 mT to 50 T at moderate excitation amplitudes. It can be used in harsh environments under mechanical vibrations and low temperatures. The device has a resonant frequency around 5 kHz, a resolution of 10 mT, and a power consumption of few milliwatts. The device needs high current magnitudes thus increasing the temperature and deformation at the silicon microbeam, with a possible resonant frequency shift.

Another example of magnetic sensor based on MEMS technology and having an optical readout has been reported by Wickenden et al. (2003).

Ren et al. (2009) reported on a resonant device exploiting the capacitive readout. The magnetic field sensor has been fabricated by using conventional MEMS technology and silicon-to-glass anodic bonding process. The device consists of a low-resistivity silicon plate suspended over a glass substrate by two torsional beams, as shown in figure 5. This silicon plate acts as electrode of sensing capacitances. Au capacitance plates are fabricated on the glass substrate and a multi-turn coil (Cr and Au layers) is deposited on silicon-plate surface. The Lorentz force causes an oscillating motion of silicon plate around the torsional beams, which produces a capacitance shift between the Au electrodes and the silicon plate. A capacitance detection circuit measured the capacitance change that depends on the magnitude and the direction of the external magnetic field. This sensor required a vacuum

packaging to increase its performance. For a pressure of 10 Pa and 150 mV driving voltage amplitude, the microsensor has a resolution of 30 nT in the linear range from 3 μT to 30 μT, a sensitivity of 481 mVT^{-1}, a resonant frequency close to 1380 Hz, and a quality factor around 2500. Nevertheless, it presented a non-linear response from 0 to 3 μT.

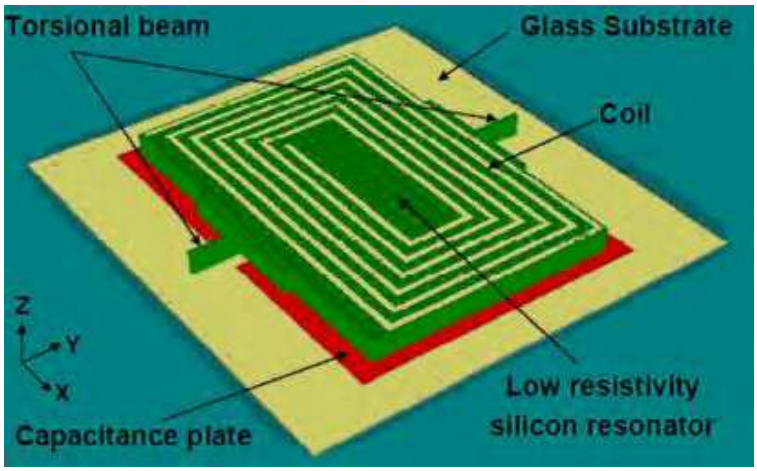

Fig. 5. Schematic design of the resonant magnetic sensor exploiting the capacitive sensing and reported by Ren et al. (2009).

Brugger et al. (2009) reported on a complex magnetic field sensor with a size of 7.5 mm × 3.2 mm, consisting of an electrostatically driven silicon resonator characterized by interdigitated combs for electrostatic excitation and capacitive detection, an amorphous magnetic concentrator and a pair of planar coils. It requires a complex fabrication process combining MEMS technology based on a silicon-on-insulator (SOI) substrate, the epoxy-resin-based attachment of a thin amorphous magnetic ribbon structured by wet chemical etching, micropatterning of the magnetic concentrator by UV-laser and vacuum packaging.. For a coil current of ±120 mA, the device offers a sensitivity of 1.91 $MHzT^{-1}$ and a resolution of 1.3 μT. Under a pressure of 10^{-5} mbar, this microsensor presents a sensitivity of 1 $MHzT^{-1}$, a resolution of 400 nT, and a quality factor around 2400. It does not need a complex feedback and modulation electronics.

J. Kyynäräinen et .al. (2008) reported on resonant micromechanical magnetometers based on capacitive detection for 3D electronic compasses. The sensors has been fabricated by exploiting aligned direct bonding of a double side polished silicon wafer and a SOI wafer. Devices operated in vacuum to reach high enough Q values. Magnetometers measuring the field component along the chip surface have a flux density resolution of about 10 $nT/\sqrt{Hz}$ at a coil current of 100 μA. Magnetometers measuring the field component perpendicular to the chip surface are currently less sensitive with a flux density resolution of about 70 $nT/\sqrt{Hz}$.

There are in the literature other works reporting on capacitive sensing-based resonant magnetic sensors (Emmerich et al. (2000), Kádár et al. (1998), Tucker et al. (2000)).

3. Fluxgate sensors

Fluxgate sensors are inductively working sensors composed of excitation and sensing coils around a ferromagnetic core for detecting static and low frequency fields.

Fluxgate sensors can detect magnetic fields up to approximately 1 mT with a maximum resolution of 100 pT. Classical fluxgate sensors are expensive and have a big size. However in recent years a great effort was devoted to manufacturing micro fluxgate sensors using microfabrication technologies. Beside the small size, the advantages of micro fluxgate sensors are small weight, low power consumption, low cost in mass production and the possibility of on-chip electronics integration. The principal disadvantage is related to the fluxgate sensor parameters dramatically degrading when reducing the core size, which leads to low sensitivity and high noise level.

The fluxgate operation principle can be illustrated with the simple layout in figure 6 (Ripka, 2001). A ferromagnetic core immersed in an external magnetic field B_x is surrounded by an excitation coil which provides an ac excitation current I. This current periodically saturates the soft magnetic material of the sensor core at a frequency twice the excitation frequency.

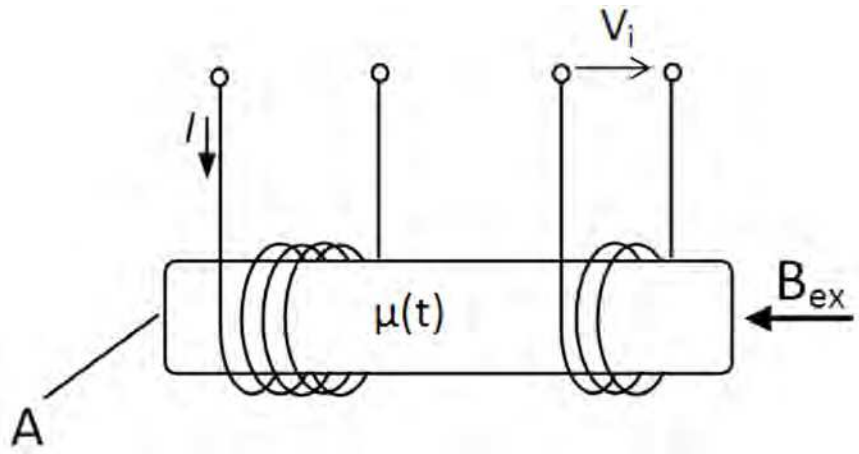

Fig. 6. The basic fluxgate principle.

A voltage in the pick-up coil (V_i) is generated due to the changing magnetic flux (Φ). From the Faraday's law:

$$V_i = \frac{d\Phi}{dt} = \frac{d(NA\mu_0\mu_r(t)H(t))}{dt} \tag{3}$$

where μr is the relative permeability, μ_0 is the vacuum permeability, N is the number of turns and A is the cross sectional area, that we consider here as a constant.

By expanding, the equation (3) becomes:

$$V_i = \frac{NA\mu_0\mu_r dH(t)}{dt} + \frac{NA\mu_0 H d\mu_r(t)}{dt} \tag{4}$$

where H is the field in the core material and is lower than the measured field H_{ex} in the open air due to demagnetization (Bozorth & Chapin (1942)):

$$H = H_{ex} - DM \tag{5}$$

where D is the demagnetising factor, $H_{ex} = B_x/\mu_0$ and M is the magnetization.

The first term in the equation (4) is the basic induction effect, and causes interference. Fluxgate operation is based on the second term, due to the variation of the core permeability with the excitation field. By considering the effect of demagnetization, the basic fluxgate equation becomes (Primdahl, 1979):

$$V_i = NA\mu_0 H_{ex} \frac{1 - D}{(1 + D(\mu_r(t) - 1))^2} \frac{d\mu_r(t)}{dt} \tag{6}$$

The output voltage is on the second harmonics of the excitation frequency, as permeability reaches its minimum and maximum twice in each excitation cycle.

In accordance with the shape of the magnetic core, parallel-type fluxgate sensors fall into the categories of single core, dual core, ring-type core, racetrack type core (Ripka, 2001). The configuration of figure 6 is single core type. In order to eliminate the induction effect, a dual core configuration has been proposed, as showed in figure 7.

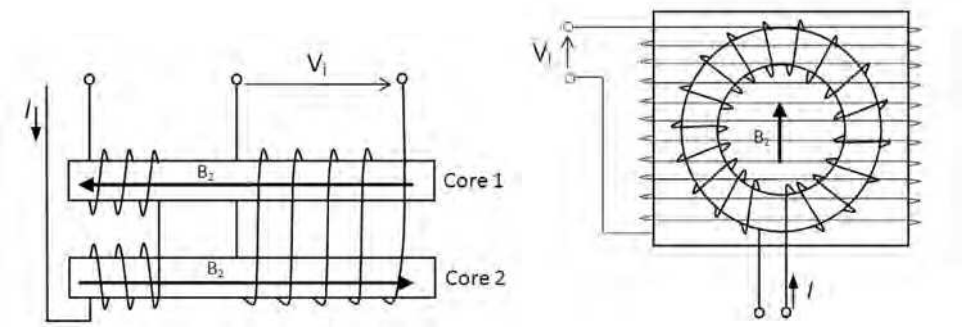

Fig. 7. Dual core (left) and ring type (right) configurations of a fluxgate sensor.

The driving coil is wound in opposite direction around the two cores, thus the induced magnetization fields are opposite in sign. If no external field is applied, the voltage induced in the sensing coil is zero in the ideal case. When an external field is present, a voltage is induced due to the differential change of the permeability (Primdahl, 1979).

High sensitivity can be achieved by increasing the number of turns N (if N is very high coil parasitic capacitance limits the sensitivity), by decreasing the demagnetization factor D or by increasing the excitation frequency, because (dHex/dt) ~ f up to frequency values that make eddy currents negligible.

Such devices can be also classified in parallel type and orthogonal type fluxgate sensors depending on the excitation field is parallel or perpendicular to the sensitive axis of the sensor.

Typically these devices contain solenoid systems wiring magnetic cores consisting of a permalloy or an amorphous material.

Figure 7 shows also the ring type configuration. The closed geometry of the ring core has a lower sensitivity but better noise performance, due to the absence of open ends.

A closed core made with oval geometry (race-track fluxgate sensor) lead to a lower demagnetization factor, then to higher sensitivity and less sensitivity to perpendicular fields.

In the orthogonal fluxgate the excitation coil is absent, and the sensor is excited directly by the current flowing through the core.

Three basic types of miniature fluxgate can be distinguished (Ripka & Janosěk, 2010): plane type sensors with flat coils, PCB-based devices with solenoids made by tracks and vias and 3D type sensors with micro solenoids.

While plane type sensors are typically fabricated by standard CMOS processes, MEMS microfluxgate sensors exploit advanced microfabrication technologies to realize three-dimensional coils or three-dimensional cores.

One of the first work which proposed MEMS technology for the development of fluxgate sensors has been reported by Liakopoulos & Ahn, (1999). In this work the authors presented a micro-fluxgate magnetic sensor based on micromachined toroidal type planar coils. In this fluxgate sensor a rectangular-ring shaped magnetic core has been chosen. The operation principle is based on the second harmonic. Excitation and sensing coils as well as permalloy magnetic cores were fabricated by a UV-LIGA thick photoresist process and electroplating techniques to realize a planar three-dimensional magnetic fluxgate sensor on silicon wafers. Excellent linear response over the range of -500 mT to +500 mT, with a sensitivity of 8360 VT^{-1} and a resolution of 60 nT was achieved with this device. The total response range of the sensor is -1.3 to +1.3 mT. The power consumption is around 100 mW for an operational frequency range of 1-100 kHz.

Woytasik et al. (2006) proposed an alternative fabrication process based on copper micromoulding to realize planar microcoils and microsolenoids for MEMS based magnetic sensors on flexible substrate. Figure 8 shows main steps for solenoid fabrication process.

The main steps for solenoids fabrication consist of the realization of the bottom conductor lines and of the air bridge by copper electrodeposition overflow. The second exposure process uses a gray-tone mask to vary spatially the exposure dose deposited into the photoresist and then to modulate the remaining photoresist thickness after development. The process ends with mould removal.

This technology has been employed for the realization of a micromachined fluxgate sensor (Wu & Ahn, 2008).

The sensor, schematically shown in figure 9, consists of a 30 μm thick electroplated permalloy core, with 56 excitation turns giving a total resistance of 2 Ω and 11 sensing turns. A sensitivity of 650 VT^{-1} was achieved for a 5.5-mm-long sensor with 14 mW power consumption. The noise is 32 nT/√Hz @1Hz , and the practical resolution is 1 μT.

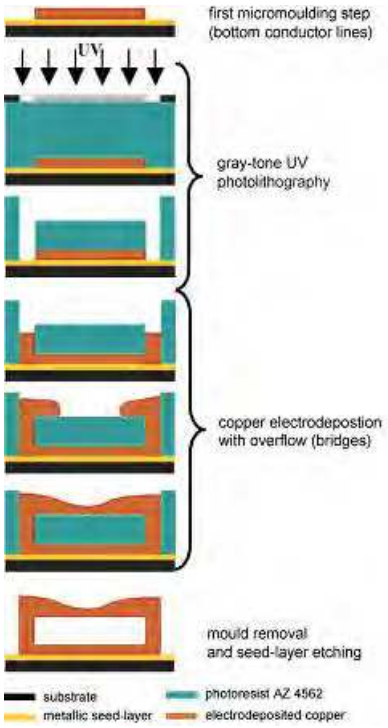

Fig. 8. Main steps of solenoid fabrication process reported by Woytasik et al. (2006).

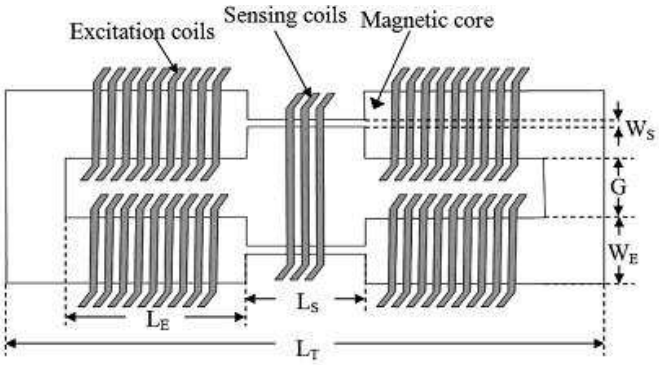

Fig. 9. Schematic view of the MEMS based fluxgate sensor proposed by Wu & Ahn, (2008).

Other examples of MEMS-based fluxgate devices have been reported by Chong Lei et al. (2009) and Kirchhoff & Büttgenbach (2010).

Most of the microfluxgate exploiting MEMS technologies are parallel sensors.

A miniature orthogonal fluxgate realized by exploiting MEMS technologies with a planar structure formed by a permalloy layer electrodeposited on a rectangular copper conductor

has been reported by Zorlu et al. (2007). The sensor structure is reported in figure 10. The sensor core is only 1 mm in length and the sensor has two flat 60 turn pickup coils.

The overall dimension of the sensor chip is 1.8 × 0.8 mm, the sensitivity is 0.51 $mVmT^{-1}$ in a linear operating range of ±200 μT. The noise was 95nT/√Hz@1Hz with an excitation power consumption of 8.1 mW.

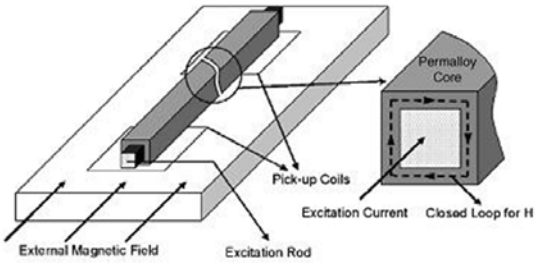

Fig. 10. Sensor structure the orthogonal microfluxgate reported by Zorlu at al. (2007).

4. Hall sensors

Hall sensors exploits Hall effect as trasduction principle to detect magnetic field. They are commonly fabricated by standard Complementary Metal-Oxide Semiconductor (CMOS) technology. In general, they are applicable in a range from 1 μT to 1 T and have a die size less than one millimeter.

These sensors can measure either constant or varying magnetic field. The frequency limit is around 1 MHz and operate well in a wide temperature range (Ripka & Tipek, 2007).

The Hall effect is based on the Lorentz force felt by charge carriers moving in a magnetic field. Figure 11 shows the schematic of the classical configuration where a thin slab of a conductor is placed in a magnetic field B_z. When a current flows in the x direction, the Lorenz force acts in the y direction, determining a charge distribution that counterbalances the force. Therefore a (Hall) voltage V_H builds up, as shown in figure 11.

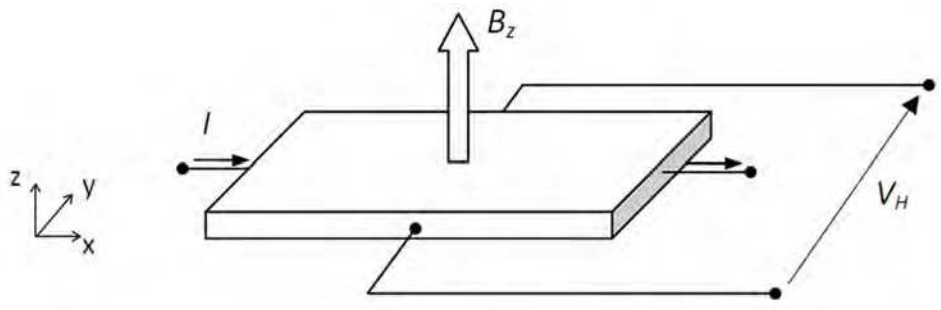

Fig. 11. Hall effect principle.

In the case of a constant current drive, the Hall voltage is given by:

$$V_H = V_{OFF} + \frac{B_z I}{e n_{2D}} \tag{7}$$

where V_{OFF} is the Hall voltage at zero magnetic field (offset voltage) and n_{2D} is the sheet charge concentration given by the product of the bulk charge concentration n and the thickness of the slab t:

$$n_{2D} = nt \tag{8}$$

If the current is constant, lower charge carriers concentration involves higher carriers speed resulting in an higher Lorentz force. Therefore low charge carrier concentration leads to high Hall voltage, thus justifying the extensive employment of semiconductor materials for Hall magnetic sensors with respect to metals.

The current related sensitivity is a key figure of merit of a Hall sensor and can be defined as:

$$S_I = \left| \frac{1}{I} \frac{\partial V_H}{\partial B_z} \right| \tag{9}$$

As the Hall voltage is related only to the z-axis magnetic field component, Hall magnetic sensors are basically uniaxial devices. Silicon based Hall sensors are widely employed, due to the suitability of integration with electronics. However, magnetic sensors based on silicon may have intrinsic limits to their sensitivity and resolution, which may limit future performance gains. In addition, they need temperature compensation circuits that can include temperature sensor and operational amplifiers (op-amps).

MEMS technology has been employed in this class of devices in order to solve some of their limitations and to find alternatives to silicon as structural material. For example polymer-based devices are interesting alternatives to silicon, particularly when the polymer materials can be functionalized for enhanced specific material properties (e.g, optical, electrical, and mechanical). Mouaziz et al. (2006) proposed the realization of SU-8 cantilevers with an integrated Hall-probe for advanced scanning probe sensing applications. To this purpose an innovative release method of polymer cantilevers with embedded integrated metal electrodes has been employed. Figure 12 shows the device fabrication process. On the silicon wafer with 0.5 μm of thermal oxide a 2 μm-thick polysilicon sacrificial layer is deposited (figure 12a). The electrodes of the Hall probe (figure 12b) and the metallic thin film electrical connections are obtained by lithographic patterning, metal deposition and liftoff (figure 12c). The device structure is obtained by lithographic patterning of two layers of SU-8 polymer: a 10μm-thick photo-structured layer for the cantilever, and a 200μm-thick layer for the chip body (figure 12d and figure 12e). The releasing method is based on dry etching of a 2μm-thick sacrificial polysilicon layer (figure 12 f).A device sensitivity of 0.05 V/AT was achieved together with a minimum detectable magnetic flux density of 9 μT/√Hz at frequencies above 1 kHz at room temperature.

Sunier et al. (2004) reported on a vertical Hall sensor with precisely defined active area fabricated by a process combining deep-RIE silicon trench etching and anisotropic TMAH silicon wet etching. The fabrication process is showed in figure 13. The main process steps are the thermal oxidation of the p-type silicon wafer (figure 13a), the definition of the trench

by dry etching, the sidewall implantation and oxidation (figure 13b), another dry etching process to deepen the trenches (figure 13c), TMAH wet etching to release the bottom of the active area (figure 13d), trench oxidation, polysilicon refill and blanket etch, contact formation and metallization (figure 13e) and finally XeF_2 etching of the polysilicon in the tranches (figure 13f).

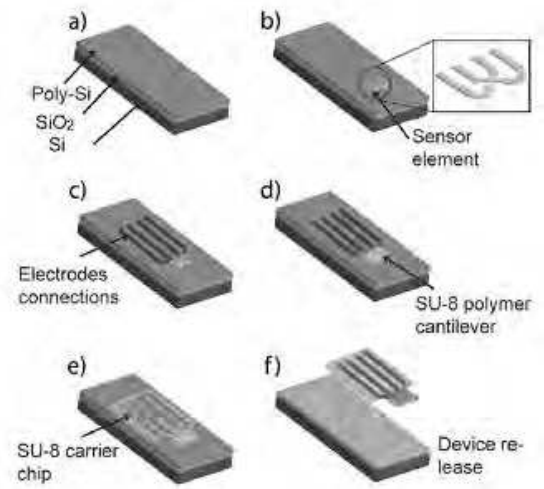

Fig. 12. Schematic illustration of the process for SU-8 cantilever with integrated electrodes reported by Mouaziz et al. (2006).

Beside a very high current related sensitivity of up to 1000 V/AT, the improved insulation from the substrate resulted in a more efficient offset compensation and then in a reduced residual offset.

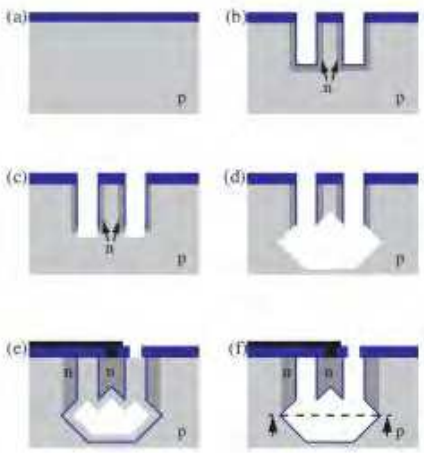

Fig. 13. Simplified fabrication process for trench Hall devices reported by Sunier et al. (2004).

Estrada (2011) proposed a three axis Hall sensor based on MEMS micromachining of SOI-wafers. Three Hall sensors embedded in a flexible polyimide carrier was obtained so that appropriate folding of the structure resulted in three Hall-probes positioned to form an orthogonally-oriented array on three faces of a millimeter-sized cube. The key fabrication process steps are as follow: (a) SOI-wafer; (b) micromachining of the active layer using either wet (TMAH) or dry (DRIE) etching; (e) patterning the Al-film needed for ohmic contacts; (f) deposition and curing of the polyimide film; g) etching of the handle wafer to reach the buried oxide film; (h) final metallization of the contact pads for possible soldering or wire bonding (figure 14).

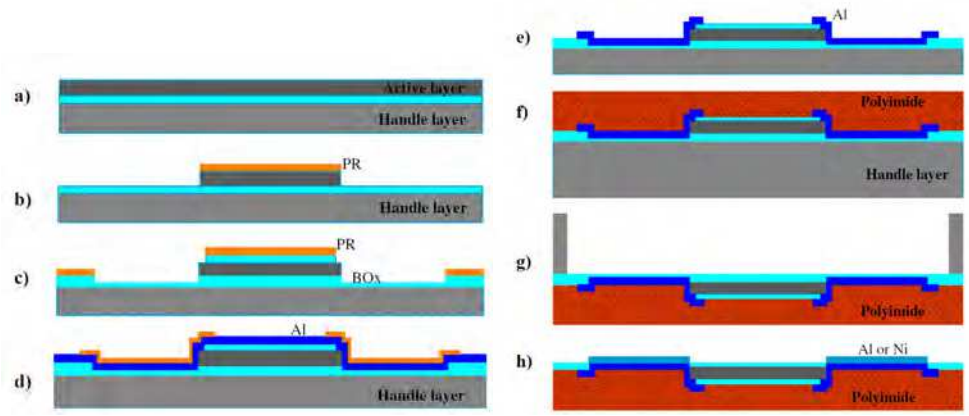

Fig. 14. Key steps for the fabrication of the three-dimensional axis Hall sensor on a flexible substrate (polyimide film) proposed by Estrada (2011).

This 3D-sensor configuration allows vector magnetic field measurements where the advantage is that all its elements have the same magnetic sensitivity of about 100 V/AT.

An integrated three axis Hall sensor based on III-V technology was fabricated by employing a micromachining technique for realizing self positioned structures (Todaro et al., 2010). The MEMS technique was applied to a GaAs-based heterostructure containing a sensing layer and a strained layer. The selective removal of a third sacrificial layer allows for the relaxation of the strained layer and the self positioning of the sensing part, which has been already processed to realize a Hall sensor element (figure 15).

The main fabrication steps are as follows: a) Epitaxial growth of a multilayer with sacrificial layer, strained layer, and sensor multilayer; (b) Photolithography and wet etching to define the mesa active region; (c) Photolithography and wet etching to define the hinge region; (d) metallization by lift off (GeAu/Ni/Au); (e) Photolithography and chemical etching to expose the edge of the sacrificial layer; (f) selective etching of the sacrificial layer and self-positioning of the structure.

Current related sensitivity of more than 1000 V/AT both for in-plane and for out-of-plane Hall sensors, demonstrates the effectiveness of this method for realizing fully integrated miniaturized high sensitivity three axis magnetic sensors.

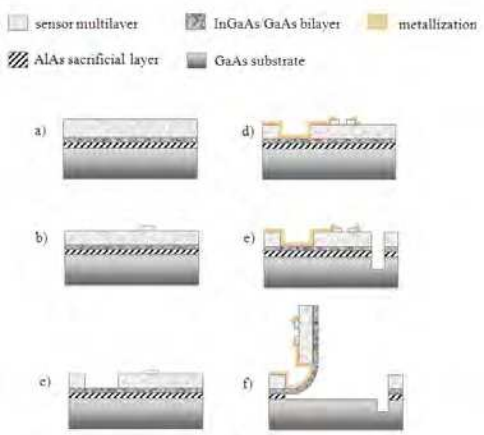

Fig. 15. Three-axis Hall sensor fabrication steps.

Figure 16 shows images of the realized three dimensional magnetic Hall sensor highlighting the out-of-plane sensor.

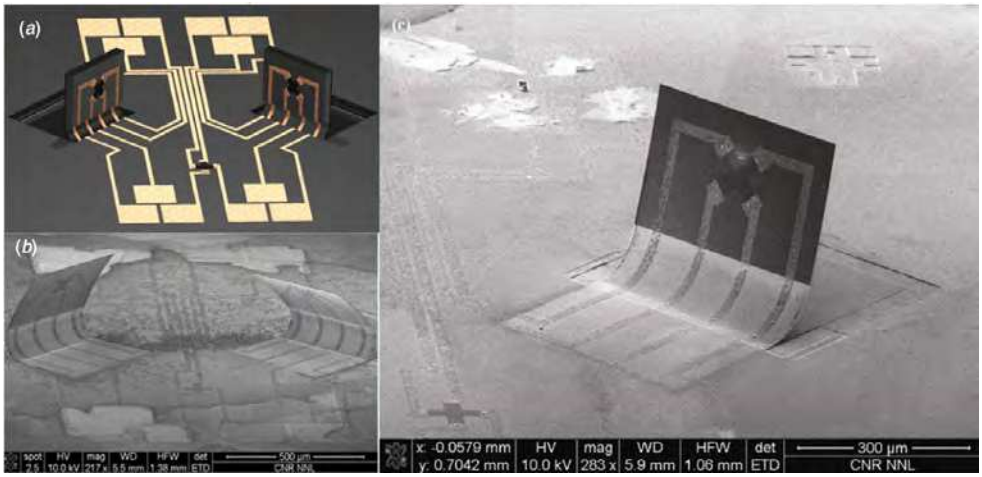

Fig. 16. Fully integrated three-axis Hall sensor reported by Todaro et al. (2010). a) a schematic of the three-axis Hall sensor; b) Image of a fabricated three axis Hall sensor; c) highlight of an out-of-plane Hall sensor acquired by scanning electron microscopy.

5. Applications

Magnetic field sensors based on MEMS technology have potential advantages with respect to conventional magnetic field sensors such as small size, light weight, compactness, lower power consumption. Additionally the MEMS technology achieves low-cost sensors by means of batch fabrication techniques and their potential integration with integrated circuits (IC) on a same substrate.

Conventional magnetic sensor classes presented in this paper have different application fields depending on their sensitivity range and minimum detectable magnetic field.

Resonant sensors have a magnetic range up to 1 T with a maximum resolution of 1nT, fluxgate sensors range spans from 100 pT to 1 mT, while Hall sensors have a sensitivity ranging from 1 μT to 1 T. Resonant sensors have lower resolution compared to fluxgate, however they present a wide sensitivity range and they could compete with fluxgate sensors into numerous applications for measuring magnetic fields.

Among the sensors presented in this paper, Hall sensors are the less sensitive devices. Their robustness and simple fabrication process justify their use in hundreds of applications.

Improvements in the microfabrication technologies combined with the employment of new and more performing materials as well as novel design solutions for devices on the microscale could enhance further the resolution, making them suitable for applications requiring very high sensitivity, such as in biomedical field and for the realization of new class of hand-held equipments. On the other hand this technology could help in new solutions for devices in applications requiring low sensitivity.

Magnetic field sensors on the microscale with moderate sensitivity, could be used for vehicle detection and recognition (Herrera-May et al. 2009). In fact vehicles moving over ground can generate a succession of impacts on the earth's magnetic field, that can be detected by means of magnetic perturbation using a magnetic sensor, and automatically recognize them by advanced signal processing and recognition method. In this context such sensors could be used for the measure of the speed and size of vehicles for traffic surveillance. Additionally magnetic field sensors can be used in systems containing accelerometers, gyroscopes and pressure devices for vehicle control applications (Niarchos, 2003). For example they can be employed in electronic stability program (ESP) systems to help vehicles to be dynamically stable in critical situations like hard braking and slippery surfaces.

Such microsensors can be employed in electronic compasses for sensing earth's magnetic field for GPS systems in order to provide more precise and instantaneous headings to aid navigation for air, ground and underwater systems. Additionally such devices can be used for global positioning systems (GPS) in cell phones due to the requirements of reduced size, low cost and low power consumption.

These magnetic field sensors find employment for the detection of compact ferrous objects (McFee et al. 1990). Such objects are of major concern in a number of applications. In environment science there is the need for portable sensors for mineral prospecting like measurements of magnetic properties of rocks, as well as detection of pipeline corrosion where geological ore inclusions generate typical peak magnetic induction in the range 1-1000 nT. In the military field such devices can be used in systems for the detection and mapping of hidden or unexplosed ordnance (mines, bombs, and artillery shells which have a peak magnetic induction in 10-1000 nT range) as well as for detection of armored vehicles (10000 nT) or submarines (1-10 nT). The performance of these systems can be enhanced by using two or three dimensional array of sensors. This could give additional informations on the size and the depth of the buried objects.

Another application of these sensors is in non-distructive testing for a variety of evaluations including medical implants and aircraft structures, the detection of cracks and corrosion in metals. Archeology is another field requiring systems including magnetic field sensors to resolve non-invasively details, the wide range of artifacts (1-1000 nT magnetic induction range) and cultural objects. This field requires also new means of mapping prehistoric and historic sites in three dimensions rather than traditional two-dimensional methods.

High sensitivity and high resolution magnetic sensors are needed in systems for medical diagnostics. Microfluxgate sensors based on MEMS technology can be employed to build cheap and portable systems for locating metallic foreign objects in the human body (Jing et al. 2009).

Ripka, (2004) showed that fluxgate sensors can be used for mapping the distribution of ferromagnetic particles in the lungs after they are magnetized by strong DC field. Medical applications requiring precise miniaturized magnetic sensors include tracking devices and systems for monitoring magnetic markers such as magnetic "biscuits" and microbeads. Magnetic biscuits can be used for functional tests of digestive tract, while microbeads are used as markers in biotechnology. New types of fluxgate microsensors are being developed for these applications (Vopalensky et al., 2003). Also Hall magnetic sensors have been employed to visualize a magnetically market diagnostic capsule in real time inside human body (Mahfuzul-Aziz, 2008). Tracking devices using fluxgate sensors can be used for monitoring the 3-D position and also orientation of a small permanent magnet which can be attached to body or medical instrument (such as catheter). Another configuration is being used for tracking the motion of the body at further distances: signals from sensors attached to the body are collected and processed.

Typically Hall magnetic devices, due to their low sensitivity are employed for position sensing, current sensing, speed detection, electronic compasses. (Lenz & Edelstein, 2006). Silicon-based Hall sensors are widely employed, due to the suitability of integration with electronics (Popovic, 1997). However, higher sensitivity sensors can be obtained with III-V technology, allowing for applications such as biomolecular function detection (Manandhar et al., 2009). Also recently, the Scanning Hall probe microscopy (SHPM) has been developed based on III-V Hall sensors, allowing for quantitative mapping of nanoscale superconducting and ferromagnetic materials (Bending et al., 2009).

Others nowadays applications such as geomagnetic measurements, environmental disturbance measurements as well as navigation systems demand for Hall miniaturized devices capable of measuring the vector magnetic field. Beside the cumbersome solution of mounting three Hall sensors with their sensitive axis orthogonal to each other, integrated three axis devices have been developed by employing silicon technology and the so called vertical Hall effect (Schott & Popovic, 1999). However these are often characterized by either different sensitivity for each component of the magnetic field (Schott et al., 2000), or by a cross-sensitivity among the direction-components (Popovic, 1999). Furthermore, offset compensation of vertical Hall element is more difficult than in the case of lateral (planar) Hall elements. In this context new materials and device configurations could open the way to realize reliable vector magnetic field sensors to be applied in different fields.

6. Conclusion

In this paper the authors described current research status in magnetic field sensors focusing on devices fabricated by exploiting MEMS technologies. The paper presents advances in some classes of devices such as resonant sensors, fluxgate sensors and Hall sensors that take advantages from these technologies. The authors focused on the description of such microsensors including operation principle, example of realized devices, highlighting the involved fabrication technologies. Possible applications of this new class of compact devices has also been reported.

7. Acknowledgment

This work was partially supported by FIRB - Hub di ricerca italo-giapponese sulle nanotecnologie.

8. References

Bahreyni, B. (2008). Fabrication and Design of Resonant Microdevices; William Andrew, Norwich, NY, USA.

Beeby, S.; Ensell, G.; Kraft, M.; White, N. (2004). MEMS Mechanical Sensors, Artech House, Norwood, MA, USA.

Bending, S.J. & Khotkevych, V.V. (2009). Scanning Hall Probe Imaging of Nanoscale Magnetic Structures. Sensor Letters, Vol. 7, No. 3, (June 2009), pp. 503-506.

Beroulle, V.; Bertrand, Y.; Latorre, L. & Nouet, P. (2003). Monolithic piezoresistive CMOS magnetic field sensors, Sens. Actuators A, Vol. 103, No. 1-2, (January 2003), pp. 23-32, ISSN 0924-4247.

Bozorth, R.M. & Chapin, D.M. (1942). Demagnetising factors of rods, J. Appl. Phys., Vol. 13, pp. 320.

Brugger, S. & Paul, O. (2009). Field-Concentrator-Based Resonant Magnetic Sensor With Integrated Planar Coils, Journal of Microelectromechanical Systems,, Vol. 18, No.6, DECEMBER (2009), pp. 1432-1443, ISSN 1057-7157.

Chang, H.; Xue, L.; Qin, W.; Yuan, G.; Yuan, W. (2008). An integrated MEMS gyroscope array higher accuracy output, Sensors 2008, Vol. 8, pp. 2886-2899.

Elwenspoek, M. & Wiegerink, R. (2001). Mechanical Microsensors, Springer-Verlag: Berling, Heidelberg, Germany.

Emmerich, H. & Schöfthaler, M. (2000). Magnetic field measurements with a novel surface micromachined magnetic-field sensor, IEEE Trans. Electron Dev., Vol. 47, No. 5, (May 2000), pp. 972-977, ISSN 0018-9383.

Estrada, H.V. (2011). A MEMS-SOI 3D-magnetic field sensor, 24th International Conference on Micro Electro Mechanical Systems (MEMS). IEEE 2011, pp. 664-667.

Herrera-May, A. L.; García-Ramírez, P.J.; Aguilera-Cortés, L.A.; Martínez-Castillo, J.M.; Sauceda-Carvajal A.; García-González, L. & Figueras-Costa, E. (2009). A resonant magnetic field microsensor with high quality factor at atmospheric pressure, J. Micromech. Microeng. , Vol. 19, No. 1, (January 2009),pp. 015016 -015026, ISSN 1057-7157.

Herrera-May, A. L.; Aguilera-Cortés, L.A.; García-Ramírez, P.J.; Manjarrez, E. (2009). Resonant magnetic field sensors based on MEMS technology, Sensors 2009, Vol. 9, pp. 7785-7813, ISSN 1424-8220.

Herrera-May, A. L.; Aguilera-Cortés, L.A.; García-Ramírez, P.J.; Mota-Carrillo, N.B.; Padrón-Hernández, W.Y. & Figueras, E. (2010). Development of resonant magnetic field microsensors: challenges and future applications, Microsensors, Intech publisher, ISBN 978-953-307-170-1.

Hull, R. Properties of Crystalline Silicon; Institution of Electrical Engineers: London, UK, 1999.

Jing, D.; Luo, E.; Shen, G.; Cai, J.; Tang, C.; Yan, Y.; Jing, B. (2009). Fast Method of Locating Metallic Foreign Body in the Human Body. The Ninth International Conference on Electronic Measurement & Instruments, ICEMI, pp. 4-843.

Kádár, Z.; Bossche, A.; Sarro, P.M. & Mollinger, J.R. (1998). Magnetic-field measurements using an integrated resonant magnetic-field sensor, Sens. Actuators A, Vol. 70 No. 3, (October 1998),, pp. 225-232, ISSN 0924-4247.

Keplinger, F.; Kvasnica, S.; Jachimowicz, A.; Kohl, F.; Steurer, J. & Hauser, H. (2004). Lorentz force based magnetic field sensor with optical readout, Sens. Actuators A, Vol. 110, No. 1-3, (February 2004), pp. 112-118, ISSN 0924-4247.

Kirchhoff, M.R. & Büttgenbach, S. (2010). MEMS fluxgate magnetometer for parallel robot application, Microsyst Technol , Vol. 16, pp. 787–790.

Kyynäräinen, J.; Saarilahti, J.; Kattelus, H.; Kärkkäinen, A.; Meinander, T.; Oja, A.; Pekko, P.; Seppä, H.; Suhonen, M.; Kuisma, H.; Ruotsalainen, S. & Tilli, M. (2008). A 3D micromechanical compass, Sensors and Actuators A, Vol. 142, pp. 561–568.

Lei, C.; Wang, R.; Zhou, Y. & Zhou, Z. (2009). MEMS micro fluxgate sensors with mutual vertical excitation coils and detection coils, Microsyst Technol., Vol. 15, pp. 969–972.

Lenz, J. & Edelstein, A.S. (2006). Magnetic sensors and their applications, IEEE Sensors Journal, Vol. 6, pp. 631-649.

Li, Y.; Zheng, Q.; Hu, Y. & Xu, Y. (2011). Micromachined Piezoresistive Accelerometer Based on a Asymmetrically Gapped Cantilever. Journal of Microelectromechanical Systems, Vol. 20, No. 1, (February 2011), pp. 83-94, ISSN 1057-7157.

Liakopoulos, T.M. & Ahn, C.H. (1999). A micro-fluxgate magnetic sensor using micromachined planar solenoid coils, Sensors and Actuators, Vol. 77, pp. 66–72.

Mahfuzul-Aziz, S.; Grcic, M. & Vaithianathan, T. (2008). A real-time tracking systems for an endoscopic capsule using multiple magnetic sensors. In Smart Sensors and Sensing Technology; Mukhupadhyay, S.C., Gupta, G.S., Eds.;. Springer-Verlag: Heidelberg, Germany, pp. 201-218.

Manandhar, P.; Chen, K.-S.; Aledealat, K.; Mihajlović, G.; Yun, S.; Field, M.; Sullivan, G.J.; Strouse, G.F.; Chase, P.B.; von Molnár, S. & Xiong, P. (2009). The detection of specific biomolecular interaction with micro-Hall magnetic sensors, Nanotechnology, Vol. 20, pp. 355501.

McFee J. E., Das Y., Ellingson R.O., (1990) Locating and Identifying Compact Ferrous Objects, IEEE Trans. Geosci. Remote Sens., Vol. 28, pag 182.

Mian, A. & Law, J. (2010). Geometric Optimization of a Van Der Pauw Structure Based MEMS Pressure Sensor. Microsystem Technologies, Vol. 16, No. 11, (November 2010), pp. 1921-1929, ISSN 0946-7076.

Mouaziz, S.; Boero, G; Popovic, R.S.; Brugger, J. (2006) Polymer-Based Cantilevers with Integrated Electrodes. Journ. Microelectromechanical Systems, Vol. 15, pp. 890

Niarchos, D. (2003). Magnetic MEMS: key issues and some applications. Sens. Actuat. A 2003, Vol. 109, pp. 166-173.

Popovic, R.S. (1997). Hall Devices for Magnetic Sensor Microsystems. IEEE Transducers'97, pp. 377.

Popovic, R.S. (1999). Novel Hall Magnetic Sensors and their Applications. EUROSENSORS XIII, 13th European Conference on Solid-State Transducers, The Hague, The Netherlands, pp. 1041-44.

Primdahl, F. (1979). The Fluxgate magnetometer, J. Phys. E: Sci. Instrum. Vol. 12.

Ren, D.; Wu, L.; Yan, M.; Cui, M.; You, Z. & Hu, M. (2009). Design and Analyses of a MEMS Based Resonant Magnetometer, Sensors 2009, Vol.9, pp. 6951-6966.

Ripka, P. (2001). Magnetic Sensors and Magnetometers, Artech House, ISBN 1-58053-057-5 Boston, USA

Ripka, P. (2004). Biomedical Application of Fluxgate Sensors. Progress in Electromagnetic Research Symposium 2004, March 28-31.

Ripka, P. & Tipek, A. (2007). Modern sensors Handbook, Wiley.

Ripka, P. & Janoseˇk, M. (2010). Advances in magnetic field sensors, IEEE Sensors Journal, Vol. 10, no. 6, (June 2010), pp. 1108-1116.

Sabaté, N.; Vogel, D.; Gollhardt, A.; Keller, J.; Cané, C.; Gràcia, I.; Morante, J.R.; Michel, B. (2007). Residual stress measurement on a MEMS structure with high-spatial resolution. J. Microelectromech. Syst., Vol.6, pp. 365-372.

Schott, Ch. & Popovic R.S. (1999). Integrated 3D Hall magnetic field sensor, Transducers'99 Proc. Conf. on Solid-State Sensors and Actuators, pp. 169-71.

Schott, C.; Besse, P.A.; Popovic, R.S. (2000). Planar Hall Effect in the Vertical Hall Sensor. Sensors and Actuators, Vol. 85, pp. 111-115.

Singh, J.; Teo, J.H.S.; Xu, Y.; Premachandran, C.S.; Chen, N.; Kotlanka, R.; Olivo, M.; Sheppard, C.J.R. (2008). A two axes scanning SOI MEMS micromirror for endoscopic bioimaging. J. Micromech. Microeng. 2008, Vol. 18, pp. 025001.

Sunier, R.; Monajemi, P.; Ayazi, F.; Vancura, T.; Baltes, H.; Brand, H. (2004). Precise release and insulation technology for vertical Hall sensors and trench-defined MEMS. Sensors, Proceedings of IEEE (2004), pp 1442.

Sunier, R.; Vancura, T.; Li, Y.; Kay-Uwe, K. & Baltes, H.; Brand, O. (2006). Resonant magnetic field sensor with frequency output. J. Microelectromech. Syst., Vol. 15, pp. 1098-1107.

Tapia, J.A.; Herrera-May, A.L.; García-Ramírez P.J.; Martinez-Castillo, J.; Figueras, E.; Flores, A. & Manjarrez, E. (2011). Sensing magnetic flux density of artificial neurons with a MEMS device, Biomed Microdevices, Vol. 13, pp. 303–313.

Todaro, M.T.; Sileo, L.; Epifani, G.; Tasco, V.; Cingolani, R.; De Vittorio, M.; Passaseo, A. (2010). A Fully integrated GaAs-based three-axis Hall magnetic sensor exploiting self-posizioned strain released structures. J. Micromech. Microeng., Vol 20, pp. 105013.

Tucker, J.; Wesoleck, D. & Wickenden, D. (2000). An integrated CMOS MEMS xylophone magnetometer with capacitive sense electronics. In 2000 NanoTech, Houston, Texas, USA, 9-12

Vopalensky, M.; Ripka, P.; Platil, A. (2003). Precise Magnetic Sensors. Sensors & Actuators A, Vol 106, pp. 38-42.

Weaver, W. Jr.; Timoshenko, S.P.; Young, D.H. (1990). Vibration Problems in Engineering, 5th ed., Wiley: New York, NY, USA.

Wickenden, D.K.; Champion, J.L.; Osiander, R.; Givens, R.B.; Lamb, J.L.; Miragliotta, J.A.; Oursler, D.A. & Kistenmacher, T.J. (2003). Micromachined polysilicon resonating xylophone bar magnetometer, Acta Astronautica, Vol. 52, pp. 421-425.

Woytasik, M.;Grandchamp, J.-P.; Dufour-Gergam, E.; Gilles, J.-P.; Megherbi, S.; Martincic, E.; Mathias, H. & Crozat, P. (2006). Two- and three-dimensional microcoil fabrication process for three-axis magnetic sensors on flexible substrates, Sens. Act. A: Phys., Vol. 132, pp. 2–7.

Wu, P.-M. & Ahn, C.H. (2008). Design of a low-power micromachined fluxgate sensor using localized core saturation method, IEEE Sensors J., Vol. 8, pp. 308–313.

Zorlu, O.; Kejik, P. & Popovic, S. (2007). An orthogonal fluxgate-type magnetic microsensor with electroplated Permalloy core, Sens. Act. A, Phys., Vol. 135, pp. 43–49.

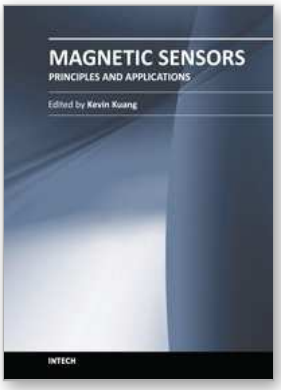

Magnetic Sensors - Principles and Applications

Edited by Dr Kevin Kuang

ISBN 978-953-51-0232-8
Hard cover, 160 pages
Publisher InTech
Published online 09, March, 2012
Published in print edition March, 2012

This book provides an introductory overview of the research done in recent years in the area of magnetic sensors. The topics presented in this book range from fundamental theories and properties of magnets and their sensing applications in areas such as biomedicine, microelectromechanical systems, nano-satellites and pedestrian tracking. Written for the readers who wished to obtain a basic understanding of the research area as well as to explore other potential areas of applications for magnetic sensors, this book presents exciting developments in the field in a highly readable manner.

InTech Europe
University Campus STeP Ri
Slavka Krautzeka 83/A
51000 Rijeka, Croatia
Phone: +385 (51) 770 447
Fax: +385 (51) 686 166
www.intechopen.com

InTech China
Unit 405, Office Block, Hotel Equatorial Shanghai
No.65, Yan An Road (West), Shanghai, 200040, China
中国上海市延安西路65号上海国际贵都大饭店办公楼405单元
Phone: +86-21-62489820
Fax: +86-21-62489821